AIAA JOURNAL
Vol. 42, No. 4, April 2004

Nonlinear Open-/Closed-Loop Aeroelastic Analysis of Airfoils via Volterra Series

Piergiovanni Marzocca*
Clarkson University, Potsdam, New York 13699-5725
Walter A. Silva†
NASA Langley Research Center, Hampton, Virginia 23681-2199
and
Liviu Librescu‡
Virginia Polytechnic Institute and State University, Blacksburg, Virginia 24061-0219

Determination of the subcritical aeroelastic response to arbitrary time-dependent external excitation and determination of the flutter instability of open/closed-loop two-dimensional nonlinear airfoils constitute the main topics. To address these problems, Volterra series and indicial aerodynamic functions are used, and, in the same context, the pertinent aeroelastic nonlinear kernels are determined. Flutter instability predictions obtained within this approach compared with their counterparts generated via the frequency eigenvalue analysis and via experiments reveal excellent agreements. Implications of a number of important parameters characterizing the lifting surface and control law on the aeroelastic response/flutter are discussed, and pertinent conclusions are outlined.

Nomenclature

a_n	=	coefficients of the Taylor series
b	=	semichord length of the airfoil
$C_{L\alpha}$	=	lift-curve slope
$C(k), F(k), G(k)$	=	Theodorsen's function and its real and imaginary counterparts, respectively
$c_{\text{hi}}, c_{\alpha i}, k_{\text{hi}}, k_{\alpha i}$	=	damping and stiffness coefficients in plunging and pitching ($i = 1, 2, 3$: linear, quadratic, cubic), respectively
h, α	=	plunging and pitching displacements
h_n, H_n	=	nth-order Volterra kernel in time, and its Laplace transformed counterpart, respectively
$I_\alpha, \hat{I}_\alpha$	=	mass moment of inertia per unit wing span and its dimensionless counterpart ($\equiv I_\alpha/10^3\pi\rho b^4$), respectively
L_a, M_a	=	total lift and moment per unit span
L_b	=	overpressure signature of the N-wave shock pulse
L_c, M_c	=	feedback control force and moment, respectively
m	=	airfoil mass per unit length
P_m	=	peak reflected pressure amplitude of the blast load
r	=	shock pulse length factor
S_α	=	static unbalance about the elastic axis
$s_j, \mathcal{L}$	=	Laplace transform variable and Laplace operator, respectively, $s_j = ik_j; i = \sqrt{-1}$
t, τ	=	time variables
U_∞	=	freestream speed
X, Y	=	input and output spectra of the system
$x(t)$	=	time-dependent external pulse (traveling gusts and wake blast waves)
$y(t)$	=	response of the considered degree of freedom (plunge h and/or pitch α)
γ_n	=	generic n-order Volterra kernel in the time domain
ρ	=	air density
τ_p	=	positive phase duration measured from the time of the arrival of the pulse
$\phi(\tau)$	=	Wagner's indicial function
ω, k	=	circular and reduced frequencies, ($\equiv \omega b/U_\infty$), respectively

Received 19 September 2002; accepted for publication 15 October 2003.

*Assistant Professor, Mechanical and Aeronautical Engineering Department. Member AIAA.
†Senior Research Scientist, Aeroelasticity Branch, Structures and Materials Competency. Senior Member AIAA.
‡Professor, Engineering Science and Mechanics Department.

I. Introduction

SUPERMANEUVERABLE combat aircraft can experience, during its operational life, dramatic reductions of the flutter speed that can affect its survivability. Moreover, the tendency to increase structural flexibility and operating speed augments the likelihood of the flutter occurrence within the aircraft operational envelope.[1,2] To prevent such an event from occurring, the development and implementation of proper active feedback control methodologies that would enable an increase of the flutter speed, enhance the aeroelastic response to external time-dependent loads, and convert the catastrophic flutter boundary into a benign boundary constitute issues of evident importance. In this sense, the nonlinear approach of lifting surfaces of aeronautical and space vehicles permits determination of the conditions under which undamped oscillations can occur at velocities below the flutter speed (in this case the flutter boundary is catastrophic) and also of the conditions under which the flight speed can be exceeded beyond the flutter instability, without catastrophic failure (in this case the flutter boundary is benign). Flutter speed, that is, the speed for which the undisturbed form of the considered structure ceases to be stable, can be determined via a linear stability analysis of the aeroelastic system. In contrast to this, the aeroelastic analysis incorporating various nonlinearities is able to address the issue of the behavior of aeroelastic systems in the vicinity of the flutter boundary.[1,2] In this sense, because of the character of the nonlinearities and of other interactive mechanical characteristics of the structure the flutter boundary can be benign or catastrophic.

The topics that will be addressed in this paper are related to the effects of nonlinearities and feedback control on the aeroelastic response in the subcritical flight speed regime and the flutter behavior of actively controlled lifting surfaces.

The methodology used is based on Volterra series[3–10] and aerodynamic indicial functions,[10–13] in which context a feedback control capability was also included.[14–16] Volterra's functional series technique[3–10] was proven to be an efficient tool for various nonlinear aeroelastic problems of systems featuring an arbitrary number of degrees of freedom.[6,7] The Volterra series approach overcomes the shortcomings facing other methods such as Hilbert's transform,[5] the phase plane method, and the method of multiple scales, which are subjected to some constrains.

In this paper, following the developments presented in Ref. 7, the Volterra series approach is applied to the active feedback control of the dynamic response of two-dimensional airfoils in an incompressible flowfield.

II. Volterra Series Approach

Aeroelastic systems are in general nonlinear. Because of their intricacy, closed-from solutions are difficult to obtain. This paper explores the idea of applying Volterra series to the closed-loop aeroelasticity of lifting surfaces. The time history of the system is represented in the form of the Volterra series, which is the summation of the first order, that is, of the linear component, and higher-order components (or nonlinear components). Although the Volterra series is an infinite series, experiments show that the information from the first few components is adequate to identify nonlinear systems in practice. Because for nonlinear systems the superposition principle is not applicable,[4] a combination of linear (TF) and high-order transfer functions (HO-TF) is used to simulate the aeroelastic response induced by unsteady aerodynamic loads and external excitations.[6] For nonlinear aeroelastic systems, the high-order transfer functions and the corresponding time histories are determined by taking the multidimensional Laplace transform of associated Volterra kernels.[6,7] For this reason those HO-TF are also called high-order Volterra kernels. Their computation will be achieved via a Mathematica® code developed by these authors.[6]

Although the transfer function is a common concept used in linear system analysis, the concept of high-order transfer function is a generalization of the linear concept applied to nonlinear dynamic systems.[5] The subcritical response of the nonlinear aeroelastic governing equations is based on the sum of multidimensional convolution integrals wherein the first kernel is linear and is analogous to the linear indicial aeroelastic function.[6] Because the flutter boundary is determined by a linear stability analysis only, the linear Volterra kernel is used for that purpose.

Corresponding to the specific type of structural, damping, and aerodynamic nonlinearities, one of the key issues is to determine the pertinent high-order Volterra kernels. When an active control capability is implemented, the Volterra kernels should incorporate the effect of the control as well. Toward the determination of the linear kernel (or linear transfer function) and the nonlinear kernels (or high-order transfer functions) that include structural/aerodynamic nonlinearities, the harmonic probing algorithm, referred to as the method of growing exponentials advanced by Bedrosian and Rice,[17] and the multidimensional Laplace transform[4–6] should be used.

A. Features of Volterra Series in Aeroelasticity

A brief description of the main features of the aeroelastic system analyzed via Volterra series follows. For more details the reader is referred to Refs. 3–5.

1. Causality

For any external load, the aeroelastic response at any instant of time does not depend on the future of the applied load. This fact implies that $h_i(\tau_1, \ldots, \tau_i) = 0$ for any $\tau_i < 0$.

2. Homogeneity

If the amplitude of the external load input would be changed, the amplitude of all of the response components would also be changed, but there would be no variation in the shape of each component waveform.

3. Finite Memory

The system memory should be finite, and the effect of an instantaneous change in the external load will tend to diminish with time. This fact is reflected in $h_i(\tau_1, \ldots, \tau_i) \to 0$ as $\tau_1, \ldots, \tau_i \to \infty$.

4. Convergence

The aeroelastic response can be approximated by a finite number of terms, implying that the series must be convergent. In general, some level of excitation would exist to cause the Volterra series to diverge. This prevents Volterra's series approach from characterizing strong nonlinear systems with high excitation components. In addition, for reducing the computational costs only a few terms can be taken into consideration.

5. Uniqueness

For a system that does comply with all of the previous necessary conditions, each Volterra kernel is independent of the excitation and unique. This property is useful. If it were possible to measure the Volterra kernels by testing the aeroelastic system with an input load of a particular type and level the Volterra series would be used to predict the response to any other input load.

B. Linear and Nonlinear Aeroelastic Kernels

In this section, a few concepts related to the Volterra series as applied to aeroelastic systems and the associated terminology are provided. The displacements, that is, plunging/pitching time histories of a nonlinear aeroelastic system $y(t)$, can be obtained as a summation of response components, which are each the result of the time-dependent external pulse $x(t)$ (due to traveling gusts or blast waves),[6,7]

$$y(t) = \sum_{n=1}^{\infty} \left[\int_{-\infty}^{\infty} \cdots \int_{-\infty}^{\infty} h_n(\tau_1, \ldots, \tau_n) \prod_{k=1}^{n} x(t - \tau_k)\, \mathrm{d}\tau_k \right] \quad (1)$$

Herein, $h(\tau_1, \ldots, \tau_n)$ stands for the Volterra kernel of the nth order, or simply nth-order kernel,[3] τ_k are time variables, while $h_1(\tau_1)$ and $h_2(\tau_1, \tau_2)$ are the linear and second-order impulse response functions, respectively.

It is assumed that $x(t - \tau_k) = 0$ for any $\tau_k < 0$, implying that the system is causal. The representation in Eq. (1) is consistent with a nonlinear system without memory, which can be described by a Taylor series:

$$y(t) = \sum_{n=1}^{\infty} a_n [x(t)]^n \quad (2)$$

Expanding Eq. (1) up to and including the third-order kernel, we obtain

$$y(t) = \int_0^t h_1(\tau_1) x(t - \tau_1)\, \mathrm{d}\tau_1 \quad (3)$$

$$+ \int_0^t \int_0^t h_2(\tau_1, \tau_2) x(t - \tau_1) x(t - \tau_2)\, \mathrm{d}\tau_1\, \mathrm{d}\tau_2 \quad (4)$$

$$+ \int_0^t \int_0^t \int_0^t h_3(\tau_1, \tau_2, \tau_3) \times x(t - \tau_1) x(t - \tau_2) x(t - \tau_3)\, \mathrm{d}\tau_3\, \mathrm{d}\tau_1\, \mathrm{d}\tau_3 \quad (5)$$

A linear aeroelastic system with memory, such as in the case in which the unsteady aerodynamic loads are present, can be described by Eq. (3), that is, via a linear convolution representation. As a limiting case of this methodology, based upon the first-order Volterra kernel $h_1(\tau_1)$, the study of the linear aeroelastic stability of the system can be carried out. Terms (4) and (5) can be viewed as the two-fold and three-fold convolutions; this implies that Eq. (1) is an infinite sum of n-fold convolution integrals. These serve to characterize the various orders of the nonlinearity.[3,4,9,10]

C. Symmetric and Symmetrized Aeroelastic Kernels

For computational reasons, it is preferable to have symmetric kernels, for example, for a second-order kernel $h_2(\tau_1, \tau_2) = h_2(\tau_2, \tau_1)$. This is always the case for open-loop aeroelastic systems.[6,7] In addition, the underlying assumption in Eq. (1) is that the kernels h_n are symmetric, which means that $h_n(\tau_1, \ldots, \tau_n)$ must have the same value regardless of the permutation of $\tau_1, \ldots, \tau_n$, that is, $h_{n\,\mathrm{sym}}(\tau_1, \ldots, \tau_n) = h_{n\,\mathrm{sym}}(\tau_{\pi(1)}, \ldots, \tau_{\pi(n)})$, where $\pi(\cdot)$ denotes any permutation of the integer $1 \ldots n$ (Ref. 4). However, because of the shift in the magnitude and phase of the resonance frequency for feedback systems the kernels of closed-loop aeroelastic systems are not, in general, perfectly symmetric. This is evident from some of the numerical simulations illustrated next.

Because a significant reduction in the number of terms is often the result of symmetric kernels and because in many cases system properties can be related to the properties of the symmetric kernel, Wiener's procedure will be pursued to symmetrize the closed-loop aeroelastic kernels.[4] It consists of permuting the subscripts of τ in all possible ways and then taking h_n to be the sum of all generic n-order kernel γ_n, that is,

$$h_{n\,\mathrm{sym}}(\tau_1, \ldots, \tau_n) = \frac{1}{n!} \sum_{\pi(\cdot)} \gamma_n\big(\tau_{\pi(1)}, \ldots, \tau_{\pi(n)}\big) \tag{6}$$

where the indicated summation is over all $n!$ permutations of the integers 1 through n. This replacement does not affect the input/output relationship.[4] In fact, considering the expression

$$\int_0^t h_n(\tau_1, \ldots, \tau_n) \prod_{k=1}^{n} x(t - \tau_k)\, \mathrm{d}\tau_k = \frac{1}{n!} \sum_{\pi(\cdot)} \int_0^t \gamma_n\big(\tau_{\pi(1)}, \ldots, \tau_{\pi(n)}\big) \prod_{k=1}^{n} x\big(t - \tau_{\pi(k)}\big)\, \mathrm{d}\tau_{\pi(k)} \tag{7}$$

it appears that, relabeling $\tau_k = \tau_{\pi(k)}$, $k = \overline{1, n}$ in every term of the summation, all terms of Eq. (7) are identical, and so summing the $n!$ terms on the right-hand side of Eq. (7) shows that the same input/output behavior is obtained. The symmetric version of the kernel can be obtained by summing over those permutations that give distinct summands and replacing $n!$ by the number of such permutations. For example, an asymmetric kernel $h_2^+(\tau_1, \tau_2)$ can be symmetrized by

$$h_2(\tau_1, \tau_2) = \tfrac{1}{2}\big[h_2^+(\tau_1, \tau_2) + h_2^+(\tau_2, \tau_1)\big] \tag{8}$$

Usually, these time-domain kernels are used in the multidimensional convolution to determine the response.

Within the present approach, for reasons to be explained next, a Laplace-based formulation is used. This formulation is based on the frequency-association technique[4,6] for nonlinear analytical systems that provides an analogue to the Laplace-transform technique for linear systems. The main advantage of this method is that it makes it easier to compute the Volterra series in the Laplace space domain, rather than in the time domain. This implies that the kernels in Laplace/frequency domains are often more useful than their time-domain counterparts. When these kernels are inverted, the result is an explicit solution for the aeroelastic response time history applicable to any time-dependent external excitation.[6] Some details, including the relation between frequency and Laplace transform enabling the conversion of the frequency-domain to time-domain descriptions, are included in Appendix A.

Focusing our attention on the linear open-/closed-loop system, the Laplace transform the linear part of Eq. (3) yields the familiar Laplace domain expression $Y(s) = H(s)X(s)$. Here $Y(s)$, $X(s)$ (the so-called output and input spectra), and $H(s)$ are the integral Laplace transforms of $y(\tau)$, $x(\tau)$, and $h(\tau)$, respectively, while $H(s)$ is the linear transfer function of the system. As a reminder, $y(\tau)$ can be also Fourier transformed, where the output and input spectra are related by $Y(i\omega) = H(i\omega)X(i\omega)$.

It is a well-known fact that for a linear system either the linear transfer function or the first kernel in time $h(\tau)$ encode all of the

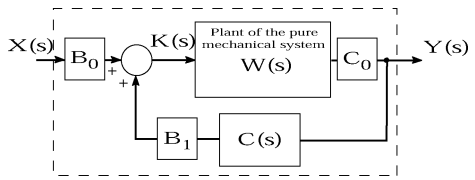

Fig. 1 Aeroelastic system represented as a plant.

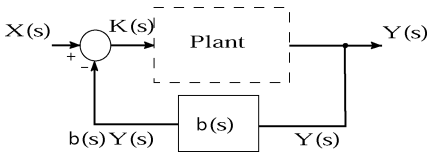

Fig. 2 Aeroelastic system incorporating a feedback control.

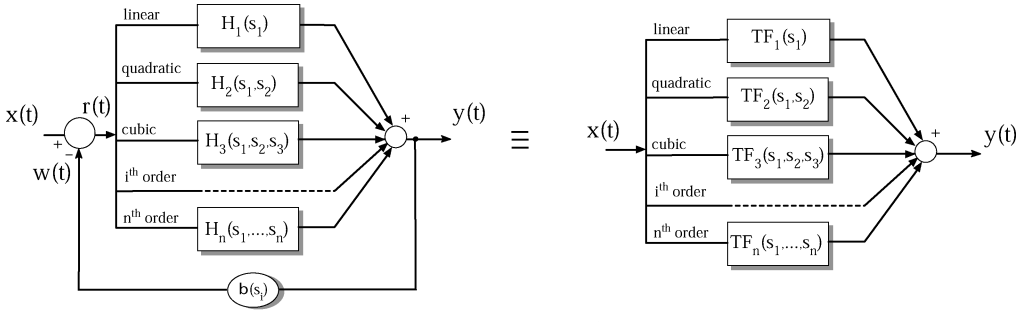

Fig. 3 Two equivalent representations of the nonlinear transfer functions of a feedback control system.

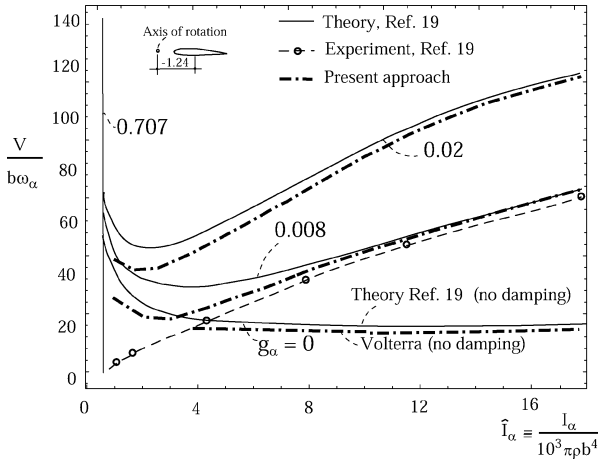

Fig. 4 Flutter speed parameter vs dimensionless inertia of an airfoil in an incompressible flow. Single-DOF pitching oscillation. The vertical line is the asymptotic limit, $\hat{I}_\alpha = 0.707$.

information about the system. This is valid for systems incorporating a feedback control capability as well. In this case, the modified first-order kernel contains the necessary information for obtaining the aeroelastic response of the controlled system.

III. Aeroelasticity of Nonlinear Airfoils

The open/closed-loop nonlinear aeroelasticity of one- and two-degree-of-freedom airfoils with structural and damping nonlinearities will be considered next. The plunging and pitching motions will be analyzed separately for an one-degree-of-freedom airfoil and the coupled plunging-pitching motion for two-degree-of-freedom airfoils.[7]

The results presented have general bearing and can be extended to systems with multiple degrees of freedom. In fact, by using the classical approach of the one-dimensional frequency response function it is possible to derive an analytical expression for the multidimensional frequency response characteristics of nonlinear systems.

The unsteady aerodynamics is assumed to be linear. A harmonic time-dependent concentrated external load is included in the analysis.

A characteristic of this approach, the linear transfer functions of the system, would exist and would be the same for any excitation (random or deterministic), such as Dirac's impulse, gusts, airblast, or sonic booms. This is because transfer functions are a characteristic of the system and are independent of the input to the system.[3–6] Then, the high-order kernels will be determined and expressed in terms of the first-order kernel.[5]

The validity of this method is based on the use of continuous polynomial-type nonlinearities. For nonlinear ordinary differential systems there are in general an infinite number of Volterra kernels. In practice, one can handle only a finite number of terms in the

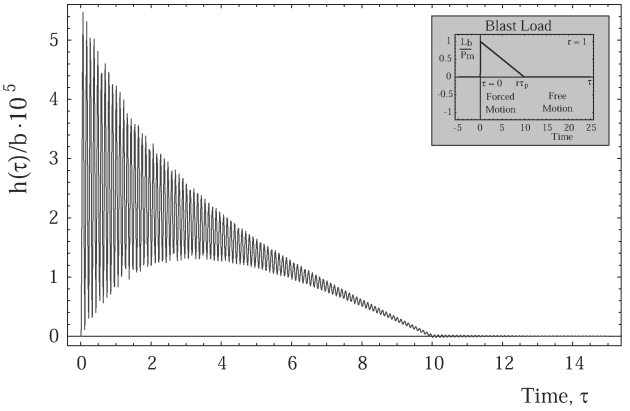

Fig. 5 Open-loop aeroelastic response of an airfoil to a blast load (as represented in the inset) via Volterra series and convolution integral $b = 1$ ft, $\rho = 1.225$ kg/m^3, $U_\infty = 1$ m/s, $m = 10$ kg, $c_{h1} = 2m\omega\zeta$, $k_{h1} = \omega^2 m$, $\zeta = 0.008$, $\omega = 60$ rad/s, $\tau_p = 10$, and $P_m = 1$. The two curves coincide.

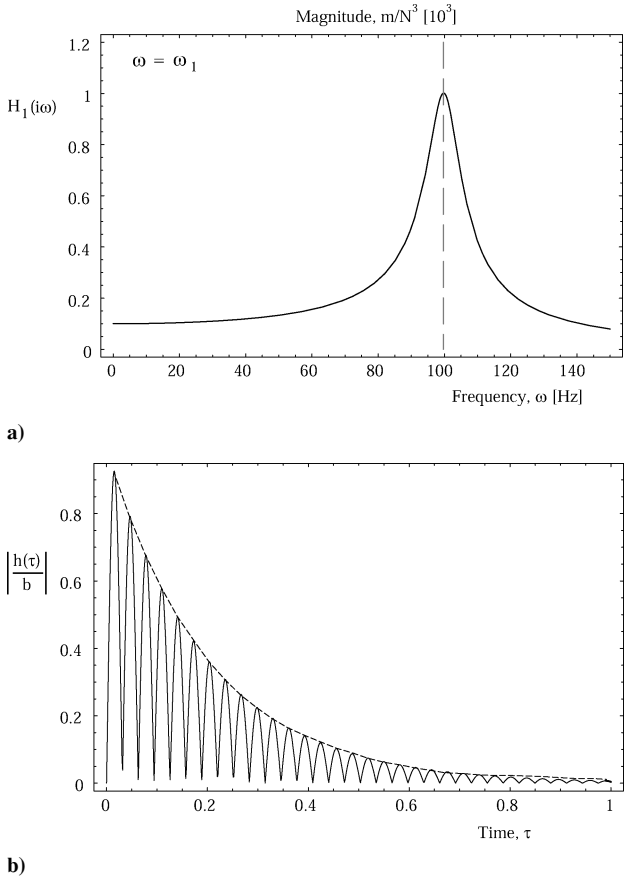

Fig. 7 First aeroelastic Volterra kernel: a) frequency and b) time representations.

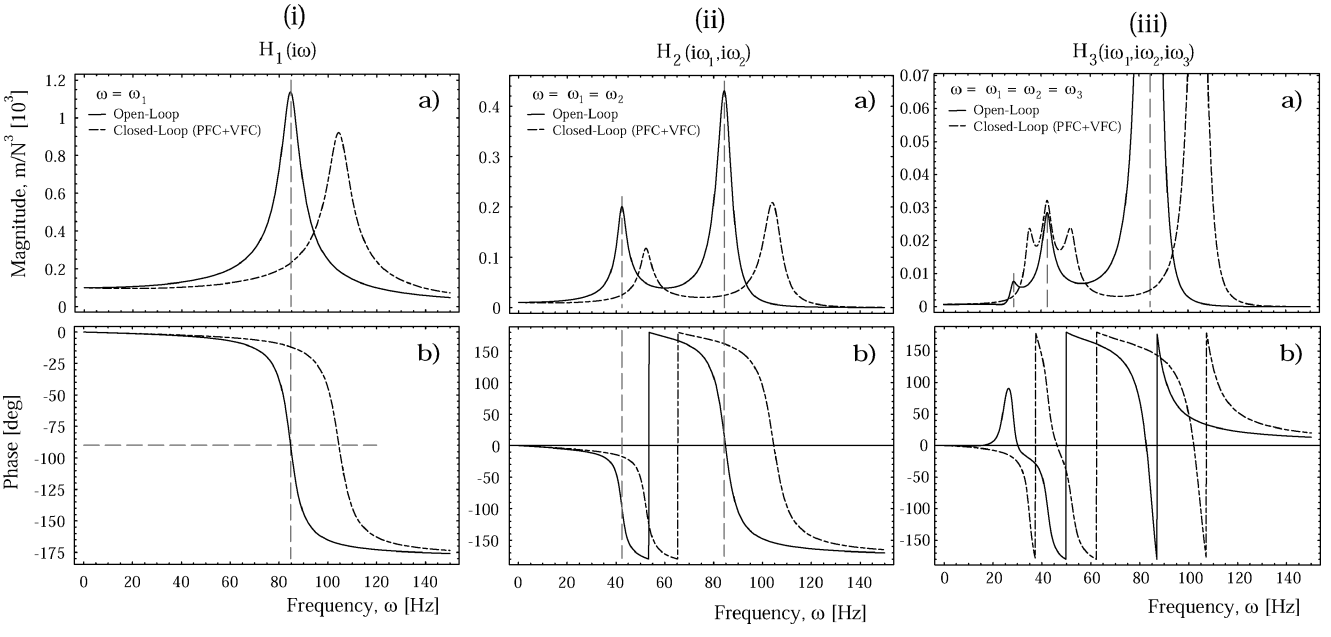

Fig. 6 Aeroelastic kernels of the open-/closed-loop aeroelastic system: (i) first order, (ii) second order, and (iii) third order, with a) magnitude and b) phase. Representation for $s_i = s$, that is, $\omega_i = \omega$, $i = 1, 3$.

series, which leads to the problem of truncation accuracy. However, Wiener suggests that the first terms of the series might be sufficient to represent the output of a nonlinear system if the nonlinearities are not too strong, for example, see Ref. 5.

IV. One- and Two-DOF Nonlinear Airfoils

A. Plunging Airfoil Motion

The open-/closed-loop, nonlinear aeroelastic equation of an airfoil featuring plunging motion subjected to an external, time-dependent load can be expressed as

$$m\ddot{h}(t) + \sum_{i=1}^{n} \left\{ c_{\mathrm{hi}}[\dot{h}(t)]^i + k_{\mathrm{hi}}[h(t)]^i \right\} = -L_a(t) + L_b(t) + L_c(t) \tag{9}$$

where i defines the degree of the considered nonlinearity.

In the numerical simulations, $i = 3$ implies that quadratic and cubic nonlinearities have been included in the structural model. In addition, m is mass parameter and c_{hi}, k_{hi} are the damping and stiffness parameters, respectively, that are associated with the damping and stiffness in plunging corresponding to the ith power. The right-hand side of these equations $L_b(t)$ denotes the external time-dependent load acting on the rigid wing counterpart,[6,12,13] and $L_c(t)$ denotes the linear active feed back control force that is expressed as

$$L_c(t) = g_p h(t) + g_v \dot{h}(t) + g_a \ddot{h}(t) \tag{10}$$

where g_p, g_v, g_a are the proportional (PFC), velocity (VFC), and acceleration (AFC) feedback control gains. In Eq. (9) the unsteady aerodynamic lift $L_a(\tau)$ is represented as a function of the plunging degree of freedom h, only:

$$L_a(t) = C_{L\alpha}\rho U_\infty b \int_0^t \phi(t-\sigma)\frac{\partial \dot{h}(\sigma)}{\partial \sigma}\,\mathrm{d}\sigma + \frac{1}{2}\rho C_{L\alpha} b^2 \ddot{h} \tag{11}$$

The noncirculatory component present in Eq. (11) has been represented in terms of a convolution integral of the indicial Wagner's function $\phi(\tau)$, which is connected with Theodorsen's function $C(s)$, via the Laplace transform as

$$C(-is) = s\int_0^\infty \phi(\tau) e^{-s\tau}\,\mathrm{d}\tau$$

This function has been included in the form of R. T. Jones's approximation.[11] A full discussion regarding the indicial function concept and its use in this approach are beyond the scope of this paper. For details related to this issue, see Refs. 6, 11–13. $C(s)$ appears in the aeroelastic feedback loop system (Fig. 1). B_0, B_1, C_0 are coefficients,[14] while the transfer function of the plant viewed as a linear mechanical system is represented by $W(s) = 1/(ms^2 + cs + k)$. When the feedback control is included in the system, the aeroelastic system can be represented as in Fig. 2.

B. Evaluation of Aeroelastic Kernels

To explain how this methodology works, the aeroelastic response of the airfoil to a harmonic or periodic time-dependent load is determined in terms of Volterra series. Let consider a periodic external excitation of the form:

$$L_b(t) = \sum_{j=1}^{n} X_j e^{s_j t} \tag{12}$$

The general procedure for identifying the aeroelastic kernels of various orders $(\overline{1, n})$ consists of considering a general input in the form given by Eq. (12) and of equating, for the generic term of nth order, the coefficients of $X_1 X_2 \cdots X_n e^{(s_1+s_2+\cdots+s_n)t}$.

This procedure was detailed in Ref. 6, where the expressions of the first three Volterra kernels of two-dimensional airfoils have been explicitly derived. As an example, the linear transfer function $H_1(s_1)$ characterizing the open-loop one-DOF aeroelastic system can be represented as

$$H_1(s_1) = \left[k_{h1} + ms_1^2 + c_{h1}s_1 + s_1\rho C_{L\alpha} b U_\infty C(k) + \tfrac{1}{2}\rho C_{L\alpha} s_1^2 b^2\right]^{-1} \tag{13}$$

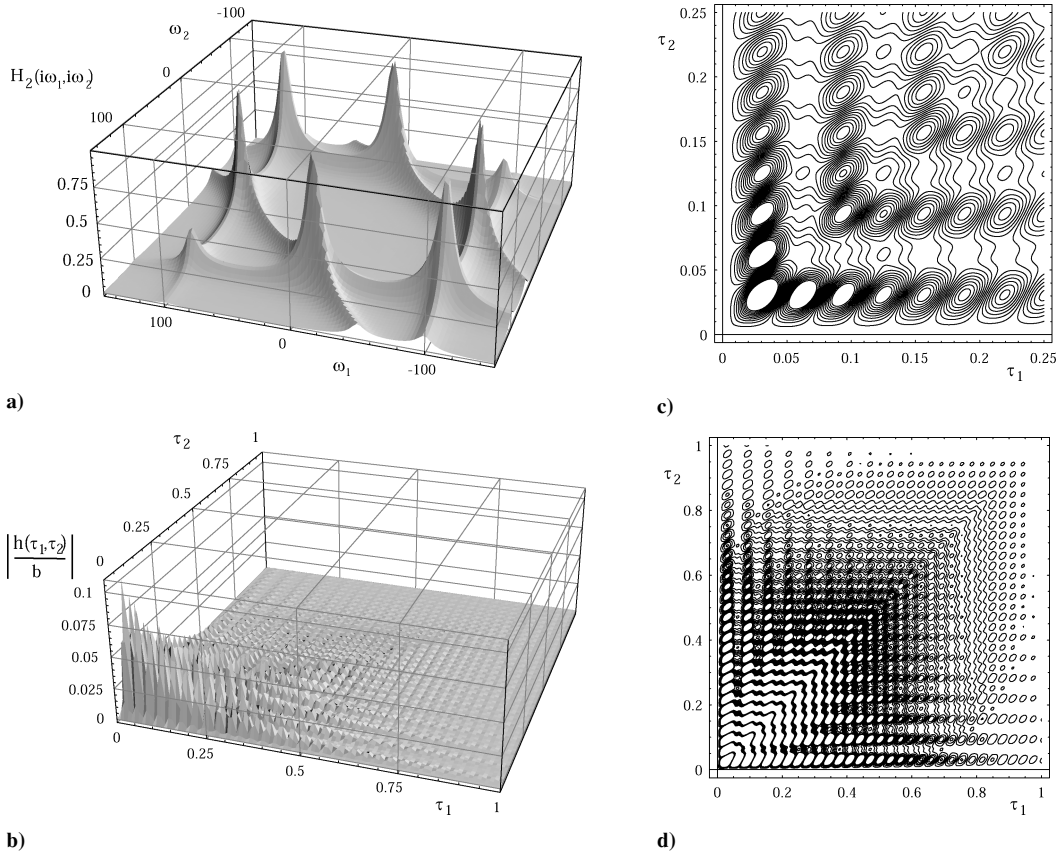

Fig. 8 Three-dimensional plot of the second-order aeroelastic kernel: a) kernel in the frequency domain, b) kernel in the time domain, and c, d) contour plots corresponding to Fig. 8b.

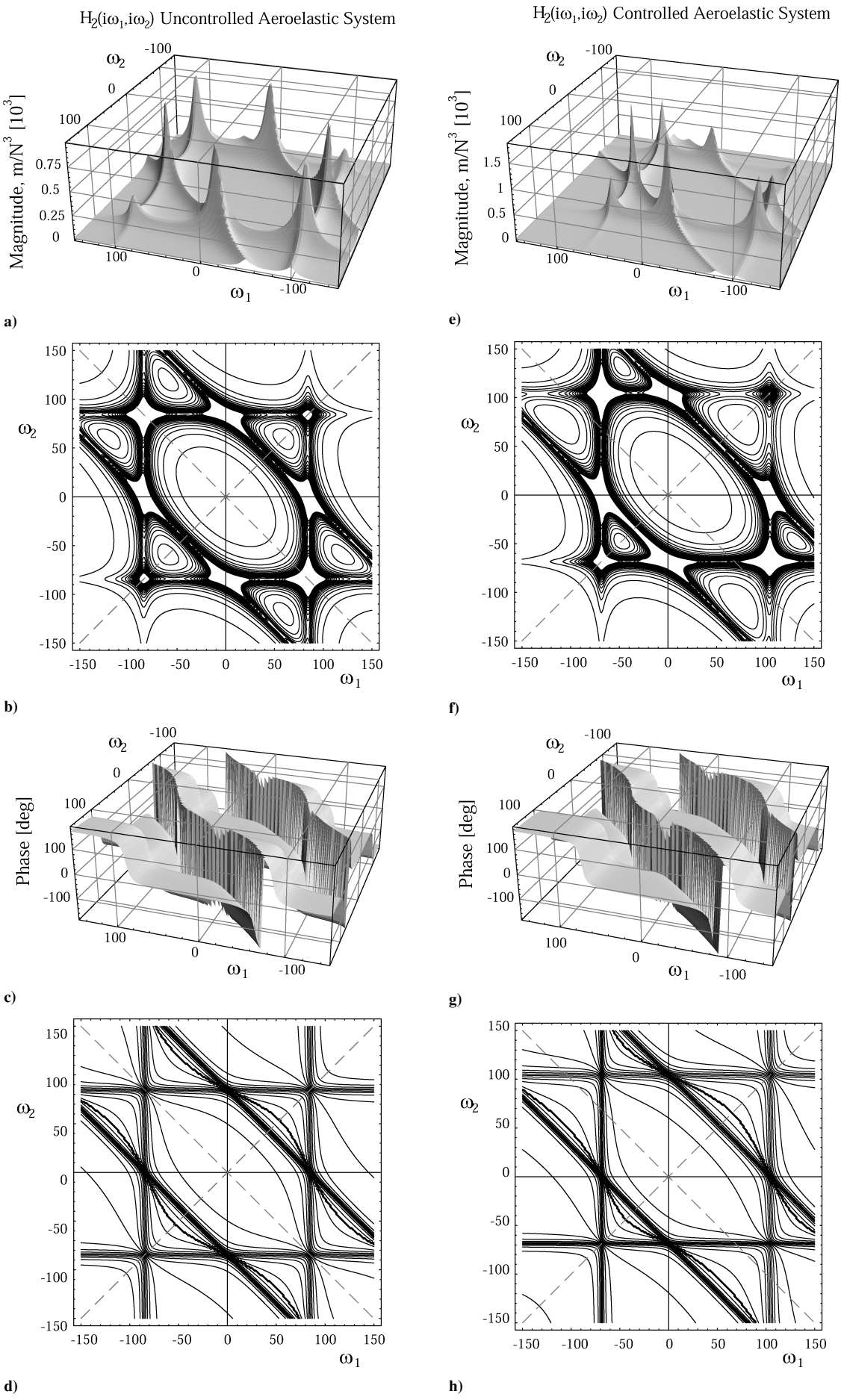

Fig. 9 Magnitude and phase representation of the second-order Volterra kernel for the a–d) open- and e–h) closed-loop aeroelastic systems.

where $k \equiv -is_1 b/U_\infty$ is the argument of the Theodorsen's function. As was already mentioned, as a general property of the system all higher-order kernels are expressed in terms of first-order H_1 (see Ref. 5–7).

C. Closed-Loop Aeroelastic Response

To actively control the aeroelastic response, control capabilities should be incorporated into the aeroelastic system. This results in a closed-loop system and implies that the response is evaluated by a sensor and is fed back to an actuator that generates a force or moment (see Fig. 2). The goals of implementing a feedback control consist of controlling the aeroelastic response behavior, increasing the flutter speed, and converting the catastrophic flutter boundary into a benign boundary.

To help understand this concept, incorporate a linear feedback control into the nonlinear aeroelastic system and address the response problem via Volterra series approach. Consider $H_1(s_1)$, $H_2(s_1, s_2)$, $H_3(s_1, s_2, s_3)$, the first three nonlinear aeroelastic kernels of the open-loop aeroelastic system.

For the present analysis, the feedback control is linear and characterized by the gain $\beta(s)$; $\beta(s)$ can be the feedback gain of one of the PFC, VFC, AFC feedback control, or combinations of these, referred to as combined feedback control, respectively.

Based on these assumptions, the linear closed-loop aeroelastic kernel $TF_1(s_1)$ is given by

$$TF_1(s_1) = \frac{H_1(s_1)}{[1 + H_1(s_1)\beta(s_1)]} = W(s_1)H_1(s_1) \tag{14}$$

From Eq. (14), when $\beta(s_1) = 0$, that is, in the case of the open loop, $H_1(s_1) = TF_1(s_1)$. $W(s_1) = 1/[1 + H_1(s_1)\beta(s_1)]$ is an error transfer function. In the specialized literature, this function is called the feedback transfer function.

From a mathematical point of view, the closed-loop nonlinear aeroelastic system that is characterized by the three transfer functions $H_i|_{i=\overline{1,3}}$ and by the feedback gain $\beta(s)$ can be seen as an open-loop system described by three new transfer functions $TF_i|_{i=\overline{1,3}}$ that are related, in some sense, with the kernels of the open-loop system and its control gains (see Figs. 3a and 3b).

To obtain the second-order closed-loop nonlinear aeroelastic kernel $[TF_2(s_1, s_2)]$, assume that the input can be expressed as $x(t) = e^{s_1 t} + e^{s_2 t}$. The output $y(t)$ can be written as

$$y(t) = TF_1(s_1)e^{s_1 t} + TF_1(s_2)e^{s_2 t} + TF_2(s_1, s_2)e^{(s_1+s_2)t} + \text{others} \tag{15}$$

Therefore, the feedback signal $w(t)$ will be

$$w(t) = \beta(s_1)TF_1(s_1)e^{s_1 t} + \beta(s_2)TF_1(s_2)e^{s_2 t} + \beta(s_1 + s_2)TF_2(s_1, s_2)e^{(s_1+s_2)t} + \text{others} \tag{16}$$

If the reference input and the controlled output are dimensionally equivalent, the error signal $r(t)$ can be expressed as $r(t) = x(t) - w(t)$, and in extended form as

$$r(t) = [1 - \beta(s_1)TF_1(s_1)]e^{s_1 t} + [1 - \beta(s_2)TF_1(s_2)]e^{s_2 t} - \beta(s_1 + s_2)TF_2(s_1, s_2)e^{(s_1+s_2)t} + \text{others} \tag{17}$$

$H_1(s_1)$ and $H_2(s_1, s_2)$ operate on the first three exponentials, respectively, to yield

$$y(t) = \{H_2(s_1, s_2)[1 - \beta(s_1)TF_1(s_1)][1 - \beta(s_2)TF_1(s_2)] - H_1(s_1 + s_2)\beta(s_1 + s_2)TF_2(s_1, s_2)\}e^{(s_1+s_2)t} + \text{others} \tag{18}$$

Comparing the expressions of $y(t)$ written in the two preceding forms, extracting the $e^{(s_1+s_2)t}$ term and using the expression of $TF_1(s_1)$, we get

$$TF_2(s_1, s_2) = H_2(s_1, s_2)\{1/[1 + H_1(s_1)\beta(s_1)]\} \times \{1/[1 + H_1(s_2)\beta(s_2)]\}\{1/[1 + H_1(s_1 + s_2)\beta(s_1 + s_2)]\} \tag{19}$$

The closed-loop aeroelastic kernel $TF_3(s_1, s_2, s_3)$ can be obtained, in a straightforward manner, by letting $x(t) = e^{s_1 t} + e^{s_2 t} + e^{s_3 t}$. The result is

$$TF_3(s_1, s_2, s_3) = \frac{1}{1 + H_1(s_1 + s_2 + s_3)\beta(s_1 + s_2 + s_3)} \times \left\{ \frac{H_3(s_1, s_2, s_3)}{\prod_{i=1}^{3}[1 + H_1(s_i)\beta(s_i)]} - 3\frac{H_2(s_1, s_2 + s_3)\beta(s_2 + s_3)H_2(s_2, s_3)}{[1 + H_1(s_2 + s_3)\beta(s_2 + s_3)]\prod_{i=1}^{3}[1 + H_1(s_i)\beta(s_i)]} \right\} \tag{20}$$

D. Stability Analysis for a Plunging Airfoil

If stability analysis is conducted in a linear framework, the aeroelastic system is characterized by the first Volterra kernel,

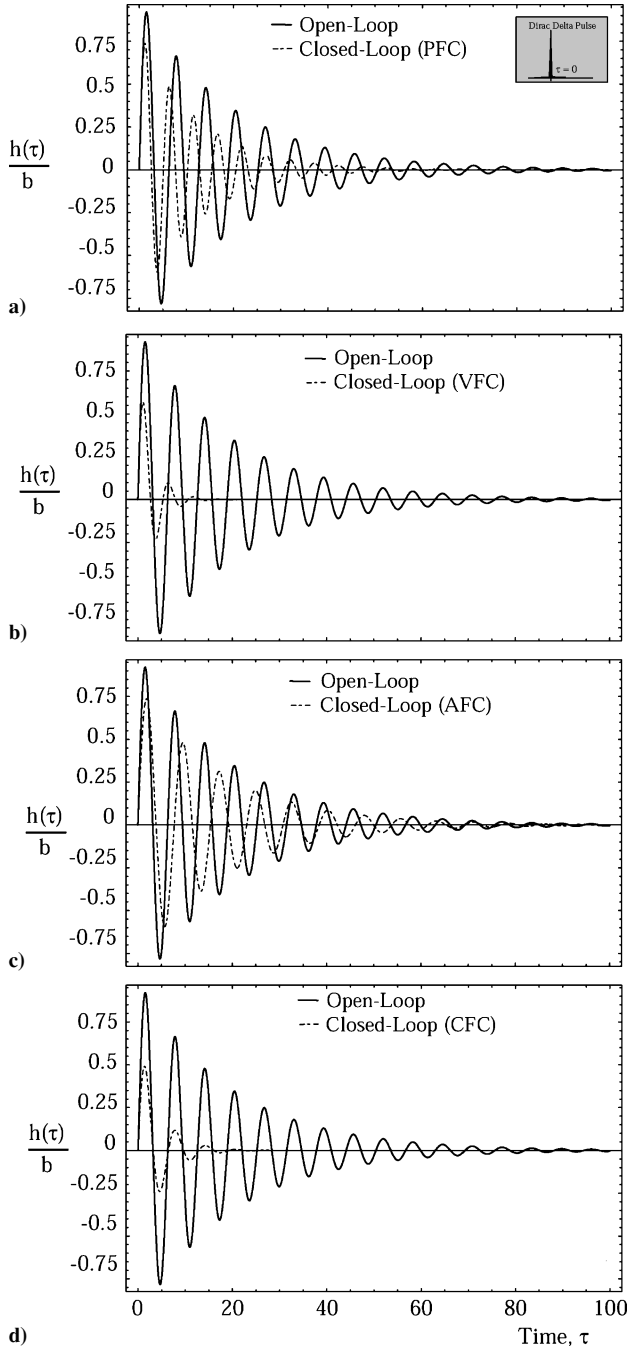

Fig. 10 Time histories of the open-/closed-loop pure plunging airfoil exposed to a Dirac delta pulse as represented in inset via selected type of feedback control.

incorporating the Wagner's function as[6]

$$H_c(s) = \left[ms^2 + c_h s + k_h + C_{L\alpha}\rho b U_\infty \Phi(s) s^2 + \tfrac{1}{2}\rho C_{L\alpha} b^2 s^2\right]^{-1} \tag{21}$$

For stability evaluations, Eq. (21) can be written in the form of a characteristic equation as

$$D_c(s) = 1/H_c(s) = 0 \tag{22}$$

Replacing $s = i\omega$, $\Phi(s)s^2$ with $C(-is)s$, where $C(k \equiv \omega b/U_\infty) = F(k) + iG(k)$ is the Theodorsen's function, and considering the real and imaginary parts of $D_c(s)$, one obtains

$$R(\omega) = -m\omega^2 + k_h + C_{L\alpha}\rho b U_\infty G(k)\omega - \tfrac{1}{2}\rho C_{L\alpha} b^2 \omega^2 \tag{23a}$$

$$S(\omega) = c\omega + C_{L\alpha}\rho b U_\infty F(k)\omega \tag{23b}$$

The stability chart for the system described in Eqs. (23) can easily be constructed. The region in the $\{c_h, k_h, U_\infty, m, b\}$ parameter space can be determined from the solution of $R(\omega) = 0$; $S(\omega) = 0$; $\omega \in (0, \infty)$.

E. Linear Pitching Airfoil Motion

As stated by Runyan,[18] the study of a single-DOF flutter is not only of an academic interest but of a practical one. A comparison of the present approach with the theoretical and experimental findings

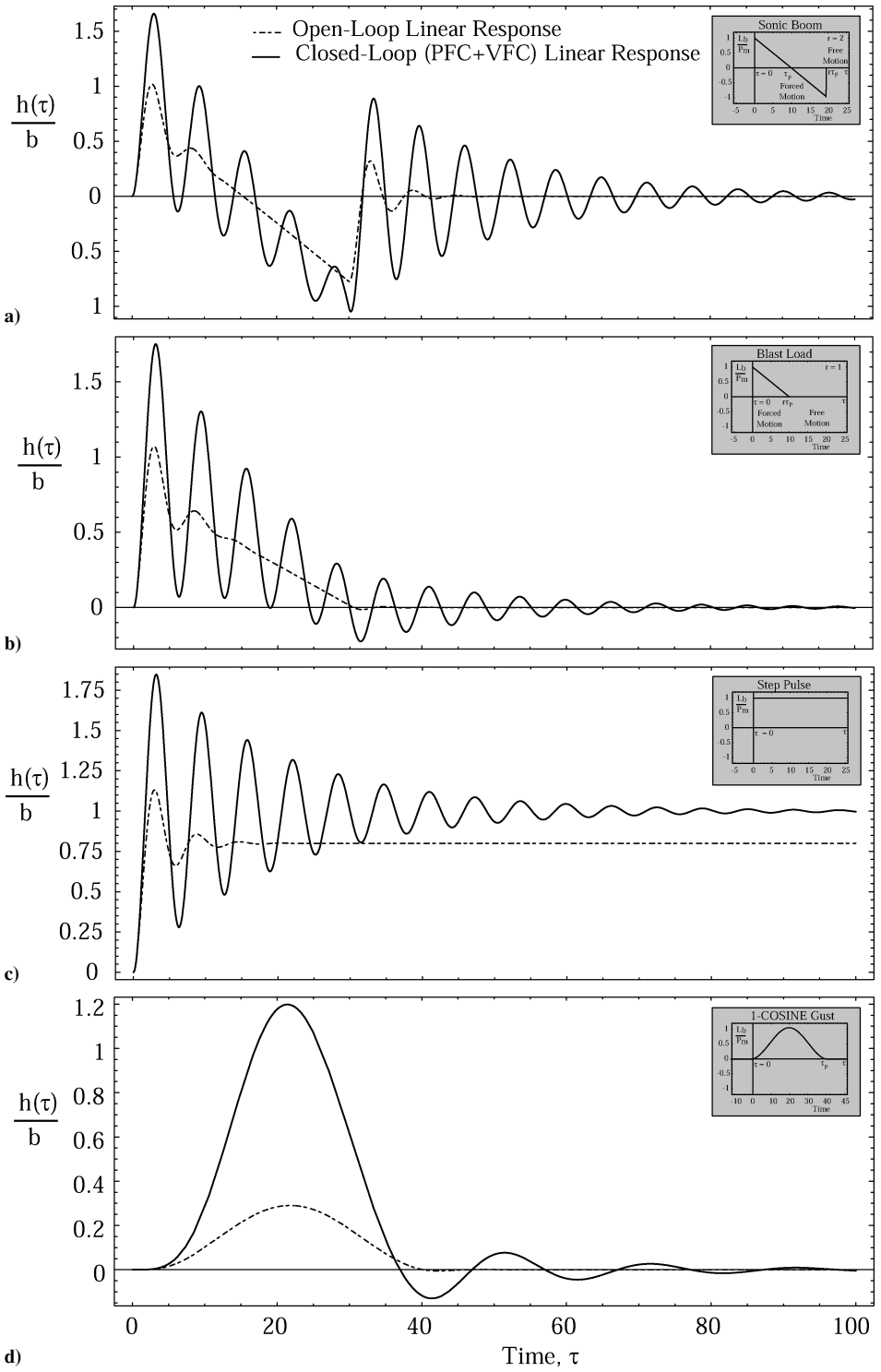

Fig. 11 Predictions of the open-/closed-loop linear aeroelastic responses of the airfoil to a) sonic boom, b) blast loading, c) sharp-edged, and d) 1-COSINE gust loads (as represented in the inset).

of Ref. 18 is presented in Fig. 4. The flutter calculations for a single-DOF pitching airfoil characterized by $I_\alpha = 0.0948$ ftlb^2/ft and $\omega_\alpha = 22.99$ for three values of the structural damping coefficient $g_\alpha = 0;0.008;0.02$ are provided. The results reveal that, for moderate to high values of the inertial parameter $\hat{I}_\alpha (\equiv I_\alpha / 10^3 \pi \rho b^4)$, the predictions via Volterra series approach are in excellent agreement with the theoretical and experimental ones. Moreover, for $\hat{I}_\alpha \leq 8$ a departure from this trend is observed, with a better agreement of the Volterra series predictions with the experimental results, as compared to those obtained in Ref. 18.

F. About the Plunging-Pitching Airfoil Motion

The aeroelastic governing equations for an airfoil with plunging-pitching coupled motion, exposed to a harmonic time-dependent external excitation, are[6]

$$m\ddot{h} + S_\alpha \ddot{\alpha} + \sum_{i=1}^{n} \left(c_{hj} \dot{h}^i + k_{hj} h^i \right) = -L_a + L_b - L_c \quad (24a)$$

$$S_\alpha \ddot{h} + I_\alpha \ddot{\alpha} + \sum_{i=1}^{n} \left(c_{\alpha j} \dot{\alpha}^i + k_{\alpha j} \alpha^i \right) = M_a - M_c \quad (24b)$$

Considering the blast load L_b as uniformly distributed in the chordwise direction, the contributing moment M_b in Eq. (24b) becomes zero. Following the steps adopted for the nonlinear one-DOF, applying a load at one frequency $L_b = X_1 e^{s_1 t}$, and expressing the plunging and pitching displacements in terms of transfer functions as

$$h(t) = X_1 H_1^h(s_1) e^{s_1 t} + X_1^2 H_2^h(s_1, s_1) e^{2 s_1 t} + X_1^3 H_3^h(s_1, s_1, s_1) e^{3 s_1 t} + \text{others} \quad (25a)$$

$$\alpha(t) = X_1 H_1^\alpha(s_1) e^{s_1 t} + X_1^2 H_2^\alpha(s_1, s_1) e^{2 s_1 t} + X_1^3 H_3^\alpha(s_1, s_1, s_1) e^{3 s_1 t} + \text{others} \quad (25b)$$

the kernels and the aeroelastic responses can be determined. Following the same steps as in the preceding sections, applying the loads $L_b(t) = X_1 e^{s_1 t} + X_2 e^{s_2 t}$, and $L_b(t) = X_1 e^{s_1 t} + X_2 e^{s_2 t} + X_3 e^{s_3 t}$, equating the terms in the forms $X_1 X_2 e^{(s_1 + s_2)t}$ and $X_1 X_2 X_3 e^{(s_1 + s_2 + s_3)t}$, the expressions for the second- and third-order Volterra kernels in the Laplace transformed space can be obtained. Some discussions related to the aeroelastic response, kernel evaluation and stability analysis for the two-DOF open-loop aeroelastic system can be found in Ref. 6. The first three aeroelastic kernels in plunging and pitching are presented in contracted form in Appendix B.

V. Numerical Results

For numerical simulations, unless otherwise stated, the parameters are prescribed as $C_{L\alpha} = 2\pi$, $b = 1$ m, $\rho = 1.225$ kg/m^3, $U_\infty = 1$ m/s, $m = 10^2$ kg, $c_{h1} = 10$ N/ms^{-1}, $c_{h2} = 10$ N/m^{2}s^{-2}, $c_{h3} = 10$ N/m^{3}s^{-3}, $k_{h1} = 10^2$ N/m, $k_{h2} = 10^3$ N/m^2, $k_{h3} = 10^4$ N/m^3, $g_p = 50$ N/m, $g_v = 50$ Ns/m, and $g_a = 50$ kg. The predictions of the linear open-loop aeroelastic responses of airfoils in an incompressible flow and exposed to a blast loading $L_b(\tau) = \lfloor H(\tau) - H(\tau - r\tau_p) \rfloor P_m (1 - \tau/\tau_p)$, based on the Volterra's series approach [using Theodorsen's function $C(k)$] and the exact solution, based on convolution integrals [using Wagner's function $\phi(\tau)$] are presented in Fig. 5. Herein τ_p denotes the positive phase duration of the pulse measured from the time of impact of the structure. For $r = 2$ the N-shaped pulse degenerates into a symmetric sonic-boom pulse[19] (in the sense that its positive phase has the same characteristics as its negative phase), and for $r = 1$ a triangular pulse that corresponds to an explosive pulse is obtained. The perfect superposition of the results constitutes a strong validation both of the accuracy of the aeroelastic model and of the power of the methodology that combines Volterra's series and the indicial function approach.

In addition, the results in Ref. 6 constitute a test of the speed of convergence of the present method. In Ref. 6, the first three approximations of the aeroelastic response to the two loads, a 1-COSINE gust and a triangular blast for a nonlinear time-varying system, are plotted for different parameters along with the "exact" response of the aeroelastic system obtained through numerical integration of the nonlinear aeroelastic equations. These comparisons reveal the rapid convergence of the approximation. For an airfoil featuring pure plunging, the magnitude and phase of the first three aeroelastic kernels are depicted in Fig. 6 as a function of the frequency, considering the representation along the diagonal of the planes (ω_1, ω_2), (ω_1, ω_3), and (ω_2, ω_3) (i.e., $\omega = \omega_1 = \omega_2 = \omega_3$). As is seen, a reduced influence on the frequency response of the third-order kernel is experienced. In addition, this figure shows the influence played by the proportional and velocity feedback controls on the kernels. It can be seen that for the present model a shift toward larger values of the frequency in the frequency response is experienced, and, at the same time, a reduction in the peaks of the kernels is obtained. The presence of nonlinearities causes harmonic excitations and sums of harmonics to appear in the response of the aeroelastic system.

Because of the nonlinear formulation, different frequencies can be expected as well. One of the advantages of the present methodology over other approaches is that this approach captures the transfer of energy between frequencies that is typical of nonlinear systems. To be more specific, one can observe that $H_1(s_1)$ produces a single frequency output in response to the simple input $e^{s_1 t}$ [see Fig. 6 (i)]. However, because the system is nonlinear $H_2(s_1, s_2)$ takes into account the terms that produce an output energy corresponding to the sum of frequencies $\omega_1 + \omega_2$ [Fig. 6 (ii)] to the input $e^{(s_1 + s_2)t}$. Similarly, the third-order nonlinear aeroelastic kernel will inject a mix of three input frequencies into the total system output [see Fig. 6 (iii)].

In Fig. 7 the magnitude of the first-order Volterra kernels for the open-loop airfoil with plunging motions in the frequency domain and its time-domain counterpart, are presented. The frequency-domain description is analogous to that based on the frequency response function (FRF) obtained within the conventional modal

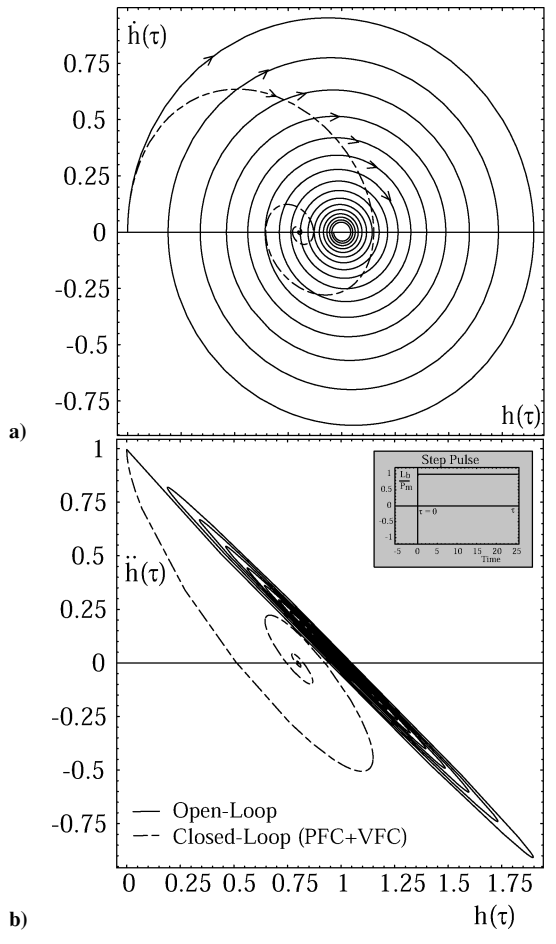

Fig. 12 Phase plots. Velocity and acceleration trajectories of the airfoil exposed to a step pulse as represented in the inset.

analysis, and, as such, the poles of the FRF identify the resonant frequencies of the system.[5]

In Figs. 8a and 8b there are three-dimensional depictions, in the frequency domain (ω_1, ω_2), of the magnitude of the second-order Volterra kernels for the open-loop airfoil featuring plunging motions (Fig. 8a) and its time-domain counterpart (τ_1, τ_2) (Fig. 8b). In Fig. 8a the kernel is depicted also for the negative frequencies ω, that is, also for the complex conjugate solution. The poles of the second-order transfer function are the poles of $H_1(s_1)$, $H_1(s_2)$, and $H_1(s_1 + s_2)$, that are dependent on the linear and nonlinear characteristic parameters. In addition, in Figs. 8c and 8d there are depicted contour plots corresponding to Fig. 8b. The time-domain representation of the second kernel shows that the kernel goes to zero very quickly, and its main contribution to the response is as a result of the terms along the diagonal $\tau_1 = \tau_2$. In Fig. 9, the magnitude and phase content of second-order kernels of the open (Fig. 9a–9d)

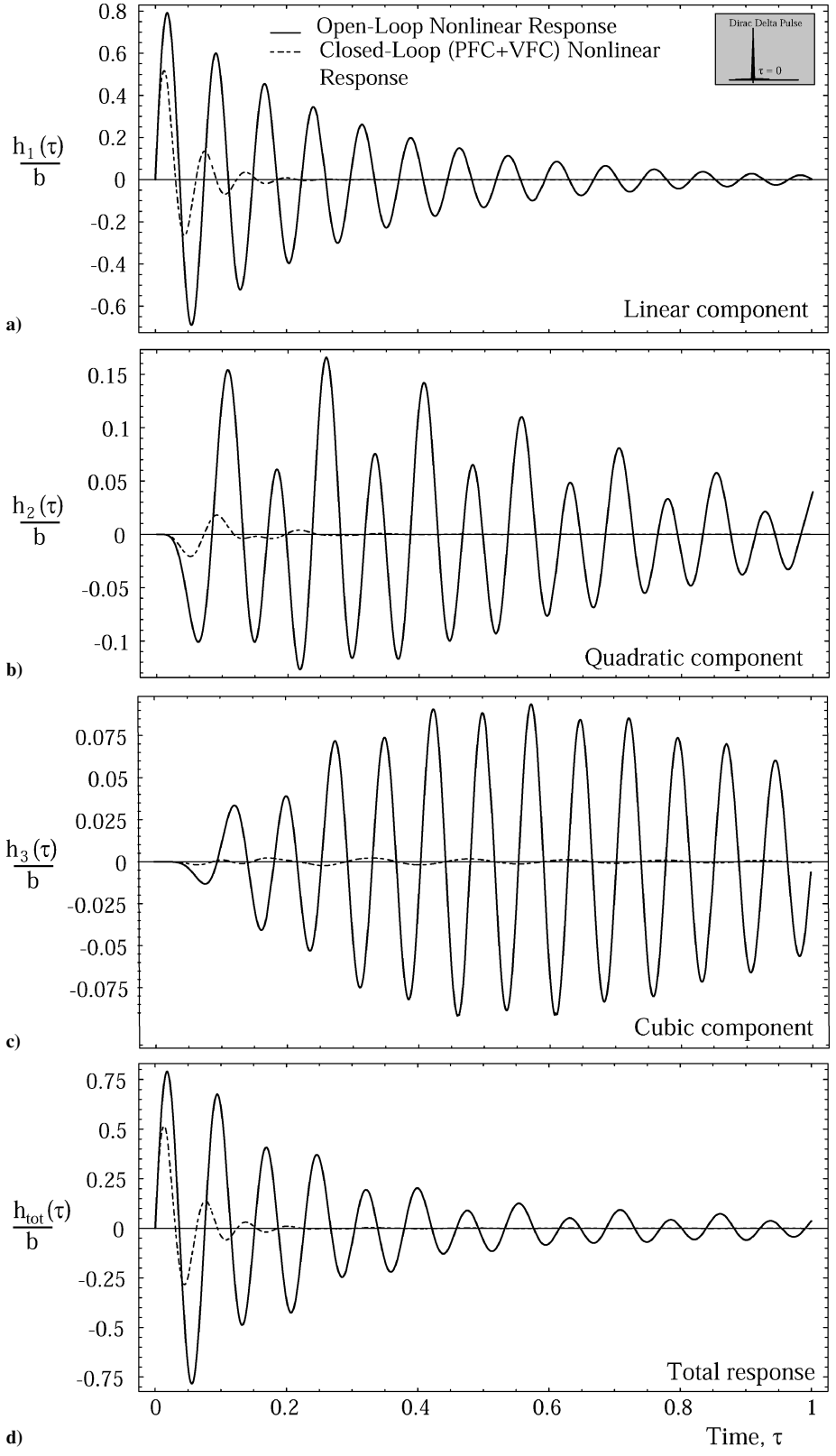

Fig. 13 Open-/closed-loop time histories of plunging displacement for the nonlinear airfoil exposed to a Dirac delta pulse via combined PFC and VFC: a) linear, Eq. (3), b) quadratic, Eq. (4), c) cubic, Eq. (5) components of the response, and d) total response.

and closed-loop (Fig. 9e–9h) aeroelastic systems are represented in the frequency domain. For the open-loop system, the contour plots (Figs. 9b and 9d) reveal the symmetry of the kernel with respect to both diagonals $\omega_1 = \pm\omega_2$. On the other hand, the conjugate symmetry of the second-order Volterra kernels can be established as $H_2(-i\omega_1, -i\omega_2) = H_2(i\omega_1, i\omega_2)$. However, for the closed-loop system (Figs. 9e and 9h) this kernel is not symmetric with respect to the diagonal $\omega_1 = -\omega_2$.

In certain nonlinear analyses we are interested in the case where $\tau_1 = \cdots = \tau_n = \tau$ (Ref. 6). This yielding to $g(\tau) \equiv h_n(\tau_1, \cdots \tau_n)|_{\tau_1 = \cdots = \tau_n = \tau}$, where $g(\tau)$ has a corresponding Laplace transform $G(s)$ (also called associated transform) in the single-dimensional Laplace transform space: $G(s) = \mathcal{L}[g(\tau)]$. The response in time can be obtained from $H(s_1, s_2, \ldots, s_n)$ by determining $G(s)$ first and evaluating the single dimensional inverse Laplace transform $g(\tau)$. This approach is called association of variable.[4,6,7]

The nonlinear aeroelastic responses in the time domain are depicted in Figs. 10–15 for the open-/closed-loop airfoil featuring the plunging degree of freedom. Figure 10 highlights the performance of various types of control on the linearized time history of the airfoil subjected to a Dirac delta pulse. It appears that the VFC constitutes, for the present case, the most efficient control law enabling one to reduce and contain the oscillations in the shortest possible time. Open-/closed-loop linear aeroelastic responses to selected types of external loading (as represented in the insets of the figures) are presented in Fig. 11, whereas in Fig. 12 velocity and acceleration trajectories are depicted for an open- and closed-loop airfoil with proportional and velocity feedback controls (PFC + VFC) to a step pulse. In Fig. 13, the first plot represents the linear impulse response that corresponds to the convolution integral for the linear analysis. The other three plots represent the components of the response as a result of the second- and the third-order kernels and the total

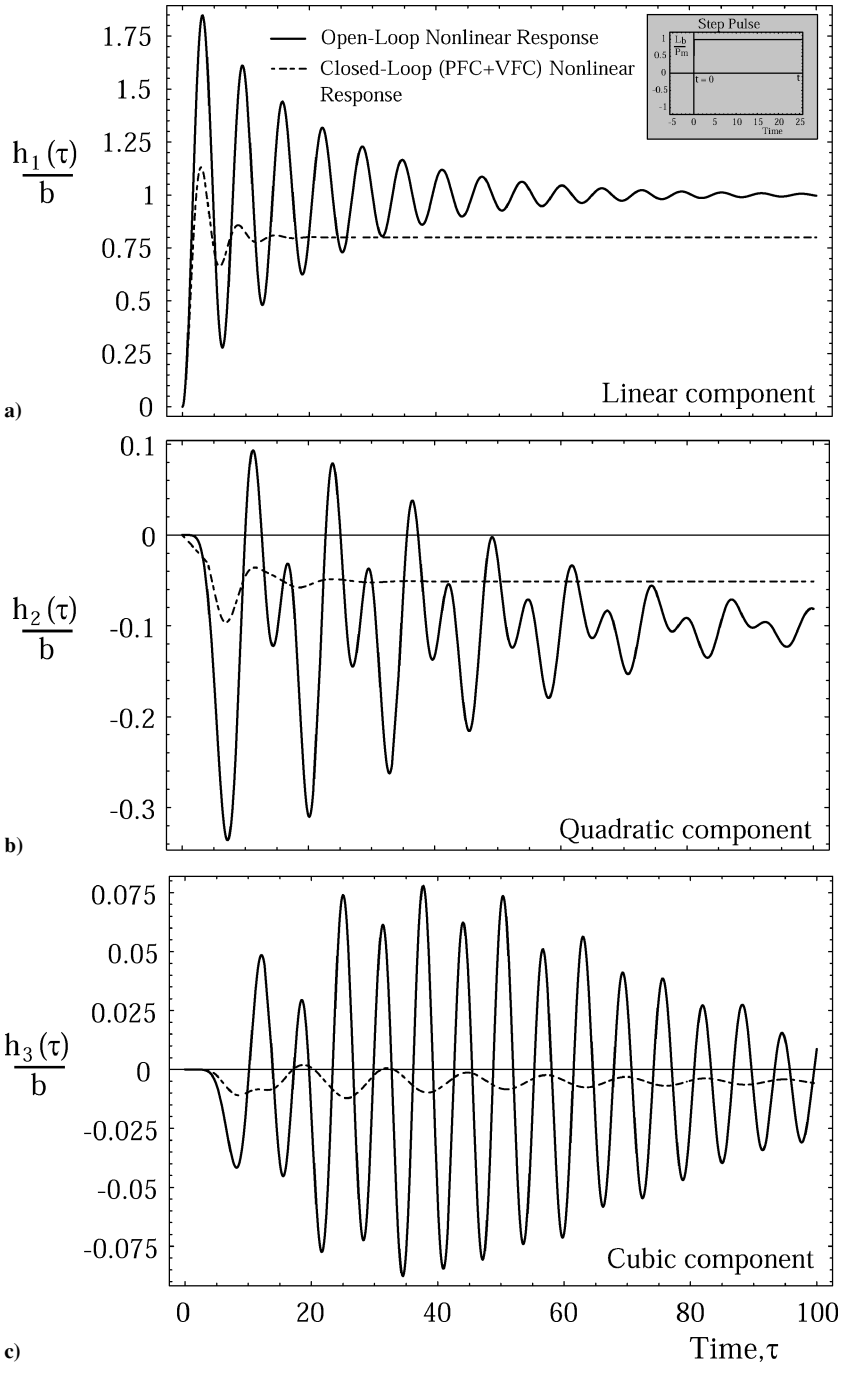

Fig. 14 Open-/closed-loop time histories of plunging displacement for the nonlinear airfoil exposed to a step pulse via combined PFC and VFC: a) linear, b) quadratic, and c) cubic components of the response.

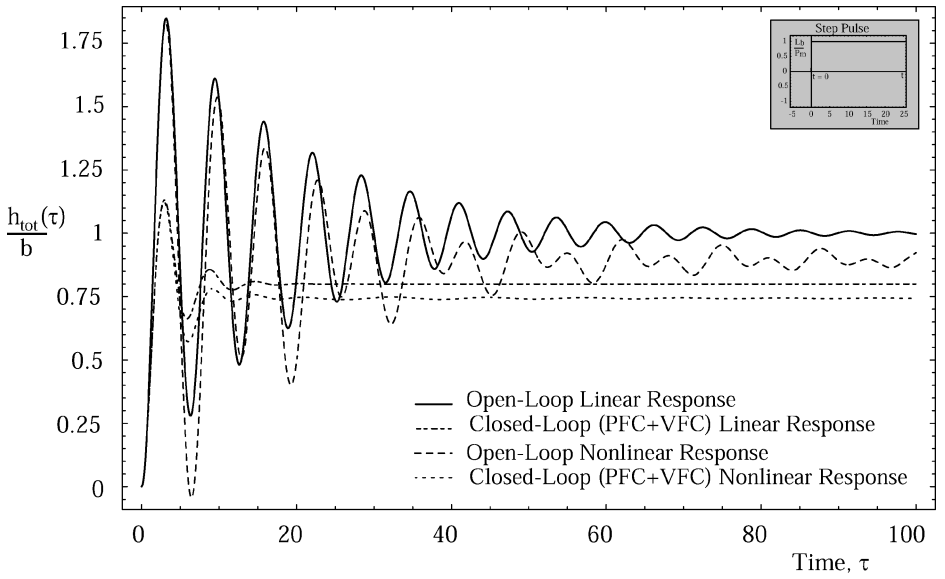

Fig. 15 Linear and nonlinear open-/closed-loop time histories of the plunging motion of the airfoil to a step pulse via combined PFC and VFC.

response as a combination of the three partial responses. The effect of the feedback control, namely a combined PFC and VFC control, is to reduce the vibrations and damp out the motion in a short time, especially to reduce the effects of the nonlinear quadratic and cubic components of the response amplitudes. A combined control law provides better results than a single control law. In addition, Fig. 13 shows the influence of the nonlinear stiffness and damping coefficients on the response.

It appears that nonlinear stiffness/damping coefficients tend to decrease the response amplitudes. Therefore, the stiffness and damping nonlinearities play a beneficial role on the subcritical aeroelastic response. Figures 14 and 15 highlight the effect of the control on the nonlinear subcritical response of an airfoil to a step pulse. Figure 14 contains the a) linear, b) quadratic, and c) cubic components of the total aeroelastic response as represented in Fig. 15. In this case, in the presence of the control the motion of the nonlinear system damps out and reaches the steady-state value in a short time. The considered control enables one to reduce and contain the oscillation in an efficient way, but is not able to reduce the response quantities to the zero value. To this end, more powerful feedback control methodologies based on rejection of disturbances should be incorporated. In addition, Fig. 15 shows that the amplitude of the nonlinear response (evaluated via the use of three kernels) is lower than its linearized counterpart, enforcing the conclusion mentioned earlier that in this case the nonlinear stiffness and damping characteristics play a beneficial role on the subcritical aeroelastic response.

VI. Conclusions

This investigation concerns the study of the open-/closed-loop subcritical aeroelastic response and flutter prediction of simple nonlinear two-dimensional airfoils in an incompressible flowfield via Volterra's series and aerodynamic indicial function. It was shown that the method based on Volterra series provides a unified and efficient way to address problems of nonlinear aeroelasticity. The approach has been extended to include an active control capability. For the linearized model, comparisons of flutter results carried out via Volterra series in conjunction with the indicial function and the U-g method have been provided. Because the unsteady aerodynamic model is presented in terms of indicial function, the formulation presented in this paper can be extended to address the open-/closed-loop aeroelastic response at various flight speed regimes and the method illustrated for one- and two-degree-of-freedom airfoils can be extended to systems with multiple degrees of freedoms, in general, and to a three-dimensional aircraft wing, in particular.

Appendix A: Laplace and Fourier Transforms

The multidimensional Laplace transform of the nth-order impulse response $h_n(\tau_1, \tau_2, \ldots, \tau_n)$ that is the nth-order transfer function is

$$H_n(s_1, \ldots, s_n) = \int \ldots \int h_n(\tau_1, \ldots, \tau_n) e^{-(s_1\tau_1 + \cdots + s_n\tau_n)}\, \mathrm{d}\tau_1 \ldots \mathrm{d}\tau_n \tag{A1}$$

As is well known, $h_n(\tau_1, \tau_2, \ldots, \tau_n)$ and $H_n(s_1, s_2, \ldots, s_n)$ provide for the nth-order homogeneous subsystem, two equivalent representations in time and Laplace-transform domain, respectively. Alternatively, the transfer function can also be defined by means of the Fourier transform, taking the n-dimensional Fourier transform of the kernel (impulse response) as

$$H_n(i\omega_1, \ldots, i\omega_n) = \int_{-\infty}^{\infty} \ldots \int_{-\infty}^{\infty} h_n(\tau_1, \ldots, \tau_n) \times e^{-(i\omega_1\tau_1 + \cdots + i\omega_n\tau_n)}\, \mathrm{d}\tau_1 \ldots \mathrm{d}\tau_n \tag{A2}$$

$H_n(i\omega_1, \ldots, i\omega_n)$ is referred to as the generalized frequency response function or system function. The close relationship between Laplace and Fourier transforms and also the fact that the n-order Volterra system will contain energy at frequencies, which are, in fact, the sums and differences of frequencies contained in the input, clearly appears from Eqs. (A1) and (A2). The Laplace transform is usually defined as one-sided $(0, \infty)$, and the Fourier transform is defined as two-sided $(-\infty, \infty)$. If a Laplace transfer function $H_n(s_1, \ldots, s_n)$ exists for $Re[s_k] = 0$, $k = \overline{1, n}$, the Fourier transfer function is given by the simple relationship

$$H_n(i\omega_1, \ldots, i\omega_n) = H_n(s_1, \ldots, s_n)|_{s_1 = i\omega_1, \ldots, s_n = i\omega_n} \tag{A3}$$

On the other hand, the response of the nonlinear system, called also output spectrum, can be expressed in the frequency domain as follows:

$$Y(f) = H_1(f)X(f) + \int_{-\infty}^{\infty} H_2(f_1, f - f_1)X(f_1)X(f - f_1)df_1 + \int_{-\infty}^{\infty}\int_{-\infty}^{\infty} H_3(f_1, f_2, f - f_1 - f_2) \times X(f_1)X(f_2)X(f - f_1 - f_2)df_2 df_1 + \cdots \tag{A4}$$

where $f_i = \omega_i/2\pi$.

Appendix B: First- and Second-Order Volterra Kernels Corresponding to Plunging-Pitching Airfoil

Terms appearing in the first and second Volterra kernels of the two degrees of freedom system are

$$A_1(s) = k_{h1} + ms^2 + c_{h1}s + s\rho C_{L\alpha} bU_\infty C\left[-\frac{isb}{U_\infty}\right] + \frac{1}{2}\rho C_{L\alpha} s^2 b^2 = \frac{1}{H_1^h(s)_{1\text{DOF}}} \tag{B1}$$

$$A_2(s) = s^2 S_\alpha + \frac{1}{2} b^2 C_{L\alpha}\rho\left\{abs^2 + s(1+2a)U_\infty C\left[-\frac{isb}{U_\infty}\right]\right\} \tag{B2}$$

$$A_3(s) = s^2 S_\alpha + \frac{1}{2} bC_{L\alpha}\rho\left\{sbU_\infty - ab^2 s^2 + U_\infty[s(2a-1) + 2U_\infty]C\left[-\frac{isb}{U_\infty}\right]\right\} \tag{B3}$$

$$A_4(s) = k_{\alpha 1} + I_\alpha s^2 + c_{\alpha 1}s + \frac{1}{16} b^2 \rho C_{L\alpha}\left\{s^2 b^2(1+8a^2) + 4s(1 - 2a)U_\infty + 4(1+2a)U_\infty\left\{sb(2a-1) - 2U_\infty C\left[-\frac{isb}{U_\infty}\right]\right\}\right\} \tag{B4}$$

$$\frac{1}{A_1(s)} + \frac{A_2(s)A_3(s)}{A_1(s)[A_1(s)A_4(s) - A_2(s)A_3(s)]} = H_1^h(s)_{2\text{DOF}} \tag{B5}$$

$$\frac{A_4(s)}{[A_1(s)A_4(s) - A_2(s)A_3(s)]} = H_1^h(s)_{2\text{DOF}} \tag{B6}$$

$$\frac{A_2(s)}{[A_2(s)A_3(s) - A_1(s)A_4(s)]} = H_1^\alpha(s)_{2\text{DOF}} \tag{B7}$$

$$\frac{H_1^h(s)_{2\text{DOF}}}{H_1^\alpha(s)_{2\text{DOF}}} = -\frac{A_4(s)}{A_2(s)} \tag{B8}$$

$$H_1^h(s)_{2\text{DOF}} = H_1^h(s)_{1\text{DOF}} - H_1^\alpha(s)_{2\text{DOF}} A_3(s) \tag{B9}$$

$$A_3(s) = \frac{H_1^h(s)_{1\text{DOF}} - H_1^h(s)_{2\text{DOF}}}{H_1^\alpha(s)_{2\text{DOF}}} \tag{B10}$$

$$B_1(s_1, s_2) = -1 + 2H_1^h(s_1)H_1^h(s_2)k_{h2} + 2H_1^h(s_1)H_1^h(s_2)c_{h2}s_1 s_2 \tag{B11}$$

$$B_2(s_1, s_2) = 2H_1^\alpha(s_1)H_1^\alpha(s_2)k_{\alpha 2} + 2H_1^\alpha(s_1)H_1^\alpha(s_2)c_{\alpha 2}s_1 s_2 \tag{B12}$$

$$H_2^h(s_1, s_2) = \frac{1}{2}\frac{B_1(s_1, s_2)A_4(s_1+s_2) - B_2(s_1, s_2)A_3(s_1+s_2)}{A_2(s_1+s_2)A_3(s_1+s_2) - A_1(s_1+s_2)A_4(s_1+s_2)} \tag{B13}$$

$$H_2^\alpha(s_1, s_2) = \frac{1}{2}\frac{B_1(s_1, s_2)A_2(s_1+s_2) + B_2(s_1, s_2)A_1(s_1+s_2)}{A_2(s_1+s_2)A_3(s_1+s_2) - A_1(s_1+s_2)A_4(s_1+s_2)} \tag{B14}$$

$$H_2^h(s_1, s_2) = \frac{B_1(s_1, s_2)A_4(s_1+s_2) - B_2(s_1, s_2)A_3(s_1+s_2)}{B_1(s_1, s_2)A_2(s_1+s_2) + B_2(s_1, s_2)A_1(s_1+s_2)} H_2^\alpha(s_1, s_2) \tag{B15}$$

$$\frac{H_2^h(s_1, s_2)}{H_2^\alpha(s_1, s_2)} = \frac{B_1(s_1, s_2)A_4(s_1+s_2) - B_2(s_1, s_2)A_3(s_1+s_2)}{B_1(s_1, s_2)A_2(s_1+s_2) + B_2(s_1, s_2)A_1(s_1+s_2)} \tag{B16}$$

$$\begin{aligned} C_1(s_1, s_2, s_3) = {} & -1 + 6(k_{h3} + c_{h3}s_1 s_2 s_3)H_1^h(s_1)H_1^h(s_2)H_1^h(s_3) \\ & + 4[k_{h2} + c_{h2}(s_2+s_3)s_1]H_1^h(s_1)H_2^h(s_2, s_3) \\ & + 4[k_{h2} + c_{h2}(s_1+s_2)s_3]H_1^h(s_3)H_2^h(s_1, s_2) \\ & + 4[k_{h2} + c_{h2}(s_1+s_3)s_2]H_1^\alpha(s_1)H_2^\alpha(s_3, s_1) \end{aligned} \tag{B17}$$

$$\begin{aligned} C_2(s_1, s_2, s_3) = {} & 6(k_{\alpha 3} + c_{\alpha 3}s_1 s_2 s_3)H_1^\alpha(s_1)H_1^\alpha(s_2)H_1^\alpha(s_3) \\ & + 4[k_{\alpha 2} + c_{\alpha 2}(s_2+s_3)s_1]H_1^\alpha(s_1)H_2^\alpha(s_2, s_3) \\ & + 4[k_{\alpha 2} + c_{\alpha 2}(s_1+s_2)s_3]H_1^\alpha(s_3)H_2^\alpha(s_1, s_2) \\ & + 4[k_{\alpha 2} + c_{\alpha 2}(s_1+s_3)s_2]H_1^\alpha(s_2)H_2^\alpha(s_3, s_1) \end{aligned} \tag{B18}$$

$$H_3^\alpha(s_1, s_2, s_3) = \frac{C_1(s_1, s_2, s_3)A_2(s_1+s_2+s_3) - C_2(s_1, s_2, s_3)A_1(s_1+s_2+s_3)}{3[A_1(s_1+s_2+s_3)A_4(s_1+s_2+s_3) - A_2(s_1+s_2+s_3)A_3(s_1+s_2+s_3)]} \tag{B19}$$

$$H_3^\alpha(s_1, s_2, s_3) = \frac{C_2(s_1, s_2, s_3)A_3(s_1+s_2+s_3) - C_1(s_1, s_2, s_3)A_4(s_1+s_2+s_3)}{3[A_1(s_1+s_2+s_3)A_4(s_1+s_2+s_3) - A_2(s_1, s_2, s_3)A_3(s_1+s_2+s_3)]} \tag{B20}$$

$$\frac{H_3^h(s_1, s_2, s_3)}{H_3^\alpha(s_1, s_2, s_3)} = \frac{C_2(s_1, s_2, s_3)A_3(s_1+s_2+s_3) - C_1(s_1, s_2, s_3)A_4(s_1+s_2+s_3)}{C_1(s_1, s_2, s_3)A_2(s_1+s_2+s_3) - C_2(s_1, s_2, s_3)A_1(s_1+s_2+s_3)} \tag{B21}$$

Acknowledgment

The partial support of this research by the NASA Langley Research Center through Grants NAG-1-01007 and NAG-1-02011 is acknowledged.

References

[1]Librescu, L., "Aeroelastic Stability of Orthotropic Heterogeneous Thin Panels in the Vicinity of the Flutter Critical Boundary," Pt. I, *Journal de Mécanique*, Vol. 4, No. 1, 1965, pp. 51–76; Pt. II, Vol. 6, No. 1, 1967, pp. 133–152.

[2]Dowell, E. H., and Ilgamov, M., *Studies in Nonlinear Aeroelasticity*, New York, Springer-Verlag, 1988.

[3]Volterra, V., *Theory of Functionals and of Integral and Integro–Differential Equations*, Dover, New York, 1959.

[4]Rugh, W. J., *Nonlinear Systems Theory, The Volterra-Wiener Approach*, The Johns Hopkins Univ. Press, 1981, pp. 1–52.

[5]Worden, K., and Tomlinson, G. R., *Nonlinearity in Structural Dynamics Detection, Identification and Modelling*, Inst. of Physics Publishing, Ltd., Bristol, England, U.K., 2001.

[6]Marzocca, P., Librescu, L., and Silva, W. A., "Aeroelastic Response of Nonlinear Wing Section by Functional Series Technique," *AIAA Journal*, Vol. 40, No. 5, 2002, pp. 813–824.

[7]Marzocca, P., Silva, W. A., and Librescu, L., "Open/Closed-Loop Nonlinear Aeroelasticity for Airfoils via Volterra Series Approach," AIAA Paper 2002-1484, April 2002.

[8]Silva, W. A., "Application of Nonlinear Systems Theory to Transonic Unsteady Aerodynamic Responses," *Journal of Aircraft*, Vol. 30, No. 5, 1993, pp. 660–668.

[9]Silva, W. A., "Reduced-Order Models Based on Linear and Nonlinear Aerodynamic Impulse Response," AIAA Paper 1999-1262, April 1999.

[10]Silva, W. A., "Discrete-Time Linear and Nonlinear Aerodynamic Impulse Responses for Efficient CFD Analysis," Ph.D. Dissertation, Dept. of Applied Science, College of William and Mary, Williamsburg, VA, 1997.

[11]Bisplinghoff, R. L., and Ashley, H., *Principles of Aeroelasticity*, Dover, New York, 1996, pp. 281–379.

[12]Marzocca, P., Librescu, L., and Silva, W. A., "Aeroelastic Response of Swept Aircraft Wings in a Compressible Flow Field," AIAA Paper 2001-0714, Jan. 2001.

[13]Marzocca, P., Librescu, L., and Silva, W. A., "Aeroelastic Response and Flutter of Swept Aircraft Wings," *AIAA Journal*, Vol. 40, No. 5, 2002, pp. 801–812.
[14]Özbay, H., *Introduction to Feedback Control Theory*, CRC Press, Boca Raton, FL, 1999, Chap. 1.
[15]Librescu, L., and Na, S. S., "Bending Vibration Control of Cantilevers via Boundary Moment and Combined Feedback Control Laws," *Journal of Vibration and Controls*, Vol. 4, No. 6, 1998, pp. 733–746.
[16]Strganac, T. W., Ko, J., Thompson, D. E., and Kurdila, A. J., "Identification and Control of Limit Cycle Oscillations in Aeroelastic Systems," *Journal of Guidance, Control, and Dynamics*, Vol. 23, No. 6, 2000, pp. 1127–1133.
[17]Bedrosian, E., and Rice, S. O., "The Output Properties of Volterra Systems (Nonlinear Systems with Memory) Driven by Harmonic and Gaussian Inputs," *Proceedings of the IEEE*, Vol. 59, No. 12, 1971, pp. 1688–1707.
[18]Runyan, H. L., "Single-Degree-of-Freedom-Flutter Calculations for a Wing in Subsonic Potential Flow and Comparison with an Experiment," NACA Rept. 1089, NACA TN 2396, June 1952.
[19]Librescu, L., and Nosier, A., "Response of Laminated Composite Flat Panels to Sonic Boom and Explosive Blast Loading," *AIAA Journal*, Vol. 28, No. 2, 1990, pp. 345–352.

E. Livne
Associate Editor